Future Foods 11 (2025) 100604

Contents lists available at ScienceDirect

Future Foods

journal homepage: www.elsevier.com/locate/fufo

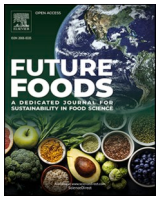

Texture engineering of aquatic protein-based products via 3D food printing

Mehdi Abdollahi [a,*], Maaike Nieuwland [c], Kjeld van Bommel [b], Laurice Pouvreau [c], Anna Ström [d], Ingrid Undeland [a]

[a] Department of Life Sciences - Food and Nutrition Science, Chalmers University of Technology, SE, 412 96, Gothenburg, Sweden
[b] The Netherlands Organization for Applied Scientific Research (TNO), Eindhoven, the Netherlands
[c] Wageningen Food & Biobased Research, Wageningen University & Research, Wageningen, the Netherlands
[d] Department of Chemistry and Chemical Engineering - Applied Chemistry, Chalmers University of Technology, SE, 412 96, Gothenburg, Sweden

ARTICLE INFO

Keywords:
3D printing
Personalized food
Protein texturization
Anisotropic texture
Marine proteins
Herring

ABSTRACT

The versatility of 3D printing in digital design and material deposition explored to adjust the internal architecture of a large portion of a protein-based food. The effect of infill density, printing pathways and their combination in customizing textural properties of model products made of proteins from fish side streams were systematically investigated. A direct correlation between the infill density and uniaxial firmness of the printed objects was found. Using different printing pathways across the Z-axis showed that parallel printing pattern can produce anisotropic textures in macroscale. This was due to a nonhomogeneous load of materials in parallel with the printing pathways, compared with its perpendicular direction in mesoscale, as revealed with micro-tomography imaging. Using cross printing pathway design was found as a way to achieve isotropic textures. Finally, using a combination of infill density and printing pathways across the X, Y axis and vertically in a non-parallel manner within a large portion of a product was proven as a new route to achieve a customizable texture profile in different parts of a single product. Altogether, our results demonstrated new possibilities for the development of protein-based products with customized heterogenous textures, closer to those in muscle, using the 3D printing technology.

1. Introduction

3D food printing is an emerging technology that allows layer by layer production of food from a predesigned, simple to complicated digital model. This provides flexibility in food production, as the digital design, the used materials, and their spatial deposition can all be changed, allowing food products to be customized and personalized, based on individual preferences concerning shape, texture and nutritional content (Lipton, 2017). Using extrusion-based 3D printing enables precise modification of the internal meso-structure (>1 mm) of foods, which defines their texture and macroscopic, or 3D, perception when using a single material (Zhu et al., 2021). This has been previously shown by changing the infill density and void fraction size or position during 3D printing of foods with relatively hard textures such as cookies (Piovesan et al., 2020), cereal-based products (Derossi et al., 2020), potato snacks (Liu et al., 2020) and dark chocolate (Mantihal et al., 2019). Infill density represent the ratio of the filled space to the total space inside the 3D-printed object and is normally expressed as a percentage. When it comes to softer food materials and pastes, changing the infill density when printing with mashed potato also resulted in changes in the instrumentally determined textural properties of the printed objects, e.g. their hardness and gumminess (Liu et al., 2018). However, still very little is known about the effects of infill density on the textural properties of products made of protein-based printing materials, especially the less explored aquatic proteins, when using extrusion-based 3D printing, where post processing is also necessary.

An essential textural feature, unique to animal muscle-based whole-cut products, is that of anisotropic structures provided by muscle fibers. This plays an important role in the sensorial perception of animal products, creating a textural properties in products that depends on the direction of the applied load (Oppen et al., 2022). Conventional seafood products, such as fish fillets, naturally offer this textural feature, but the muscle structure completely disintegrates when using the wet fractionation process for valorization of seafood side streams. Therefore, the recovered proteins and their products lack the typical fibrous structure and anisotropic texture seen in fillets. Although extrusion cooking has

* Corresponding author.
E-mail address: khozaghi@chalmers.se (M. Abdollahi).

https://doi.org/10.1016/j.fufo.2025.100604
Received 5 May 2024; Received in revised form 1 March 2025; Accepted 15 March 2025
Available online 15 March 2025

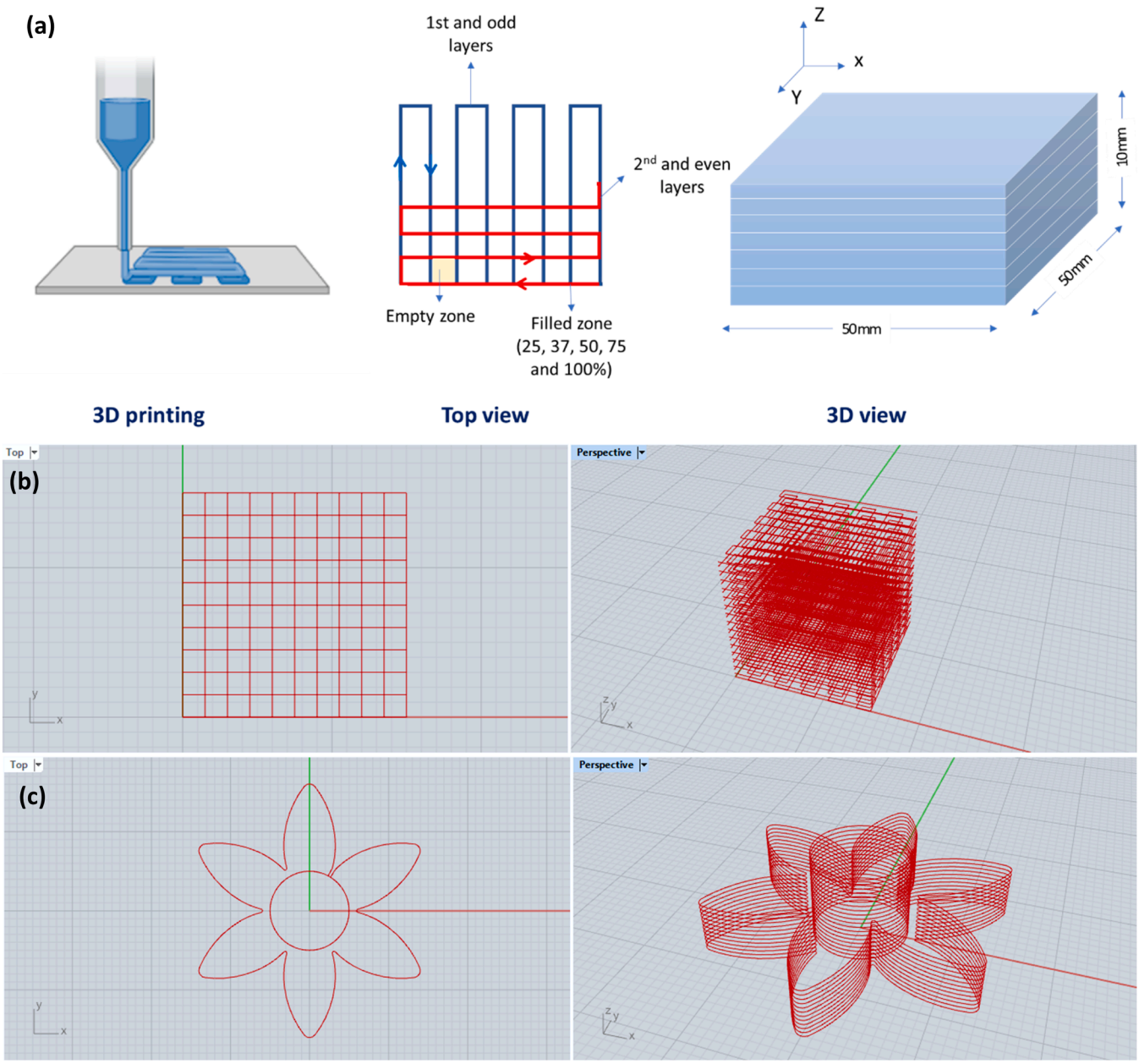

Fig. 1. Schematic view of the designed models used for development of (a and b) cubes with different infill density and (c) the flower to investigate the ability of the material in printing more complicated objects.

been found to be efficient in the production of anisotropic structures from alternative proteins, its application cannot currently be expanded to whole-cut products and it has limitations in customizing products. Generally, the layer by layer production process used in 3D printing results in an inherent anisotropic texture in the produced products (Dadbakhsh et al., 2016; Jonkers et al., 2022). This anisotropy is apparent in the higher mechanical strength when a stress is applied perpendicularly to the vertically stacked layers, compared to loading it parallel with the layers, as was for example demonstrated for starch-based food objects created by means of a selective laser sintering-based 3D printing process (Jonkers et al., 2022). However, it has not been explored whether customized designing of printing pathways (printing filament direction) and precise alignment of mesoscale fibers (i.e. the printed filaments) deposited during 3D printing of protein pastes can contribute to achieving anisotropic textures in macroscales vertically. Here, printing pathways refer to the specific routes or patterns that the 3D printer nozzle follows while depositing material layer by layer to build the final object. These pathways are determined by the 3D model's design and the instructions generated by the slicing software, which converts the digital model into a series of instructions for the 3D printer (see Fig. 2 as an example). In addition, very little is known about the effect of printing pathways on the textural properties of protein-based 3D printed products.

Another overlooked opportunity is to use the flexibility in digital designing, provided by 3D printing, for tuning the internal structure and architecture of foods to engineer textural properties across a large portion of a single product to mimic the biological texture of a real food or even going beyond that. This potential was recently explored for the recreation of apple tissue microstructure in cereal-based snacks (Derossi et al., 2022). However, to the best of our knowledge, the potential for engineering the texture profile of a single product using protein-based inks through digital design modifications of both infill density and printing pathways together has not been explored.

The present study was aimed to explore the unique opportunity that

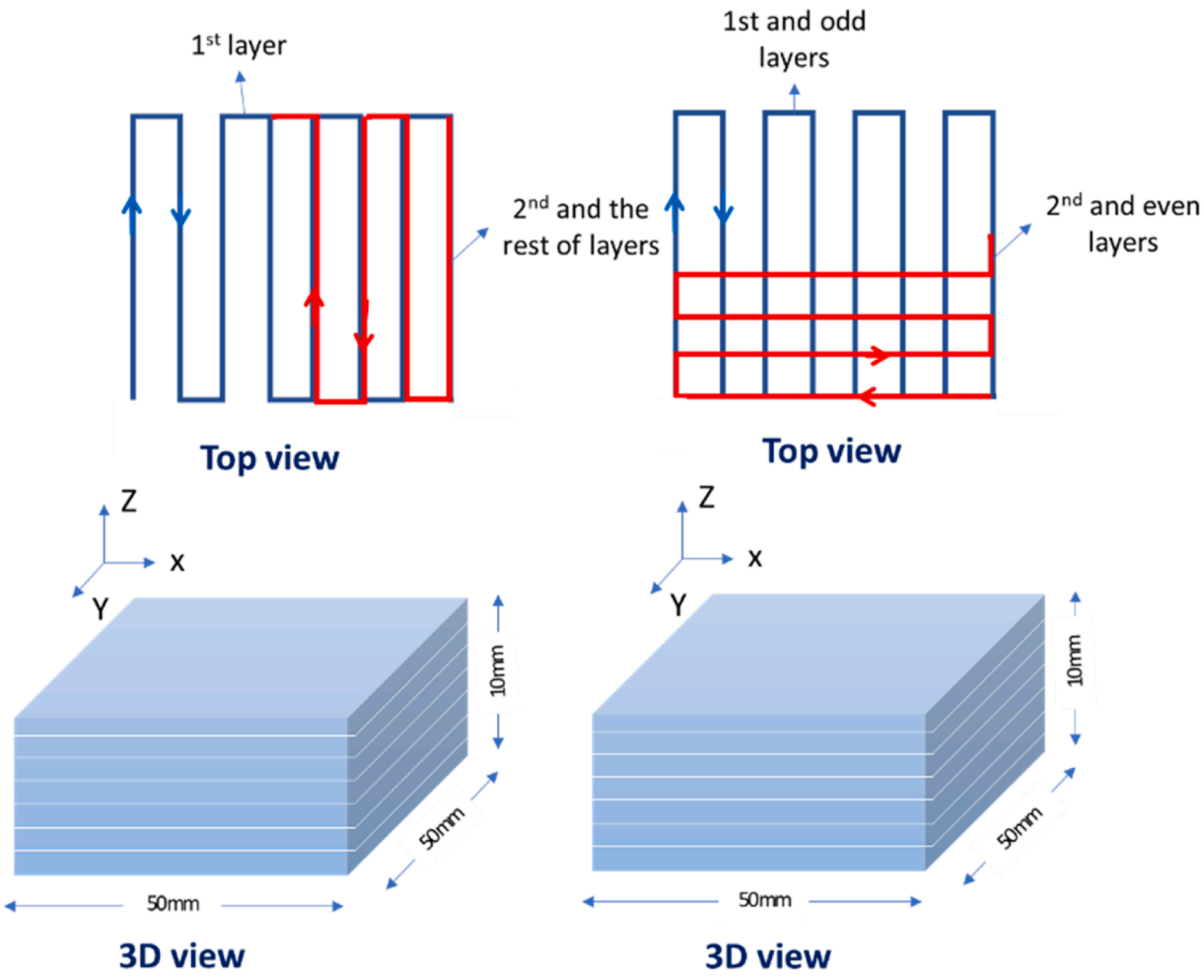

Fig. 2. Schematic view of the designed models used for development of cubes with different parallel printed pathways (left) and cross pathways (right) in all layers across the Z axis.

digital design in 3D printing technology provides to engineer new textural properties in product made of protein recovered from fish processing side streams. After optimizing the printability of the fish protein isolate with addition of pectin based on rheological properties and visual observation, the effects of infill density, printing pathways and their combination, in tuning and customizing textural properties of model seafood products made of the proteins were separately investigated. In addition, innovative ways for creating an unparallel texture profile across the X and Y axis of the 3D model products were evaluated. The possibility of developing anisotropic microstructures via proper design and alignment of mesoscale fibers was also demonstrated.

2. Materials and methods

2.1. Preparation of fish raw materials

Frame of freshly filleted Atlantic herring (*Clupea harengus*) provided by Sweden Pelagic AB (Ellös, Sweden) was transported to Chalmers University of Technology, while packed and covered with plastic bags filled with ice. The samples were then grinded using a mincer with a front plate having 4.5 mm holes (C/E22 N, Minerva Omega group, Italy). The mince was packed in plastic zip-lock bags and stored at - 80 °C until used for protein isolation.

2.2. Protein isolation from herring frame

The protein isolation from the minced samples was done using alkaline solubilization at pH 11.5 and isoelectric precipitation at pH 5.5, as explained by (Abdollahi et al., 2021). The dry matter of the isolated protein was adjusted to 20 % (protein= 85 % dry weight, fat= 7 % dry weight fat and ash = 2 % dry weight) using an extra centrifugation cycle (8000 × g for 10 min at 4 °C). Finally, its pH was readjusted to 7 using 2 M NaOH, packed and stored at - 80 °C.

2.3. Preparation of 3D printing protein-based ink

The protein isolate with 80 % moisture was defrosted under running cold tap water until reaching a core temperature of 0 °C and then chopped for 1 min using a mini chopper which was used as the control in the first part of the study. To explore the possibility of improving the printability of the paste in terms of accuracy and resolution, 0.5 % of pectin (high methoxyl pectin from citrus peel, with a molecular weight of 23 kDa to 71 kDa, Galacturonic acid ≥74.0 % (dried basis), Sigma Aldrich, Germany) was directly added as a powder to the protein and chopping was continued for 2 more min. The pastes with and without pectin were finally stuffed into a 30 mL plastic syringe using a stainless-steel mold designed for filling the syringes, and filled syringes were used immediately for 3D printing.

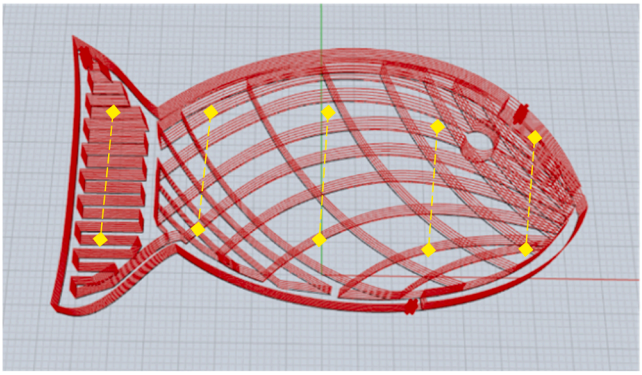

Fig. 3. Schematic view of the designed model representing a fish. The design has a texture profile along its shape, as a result of different infill densities and printing path directions. Yellow dashed lines show the locations across the fish which has been subjected to uniaxial compression test for texture analysis.

2.4. Rheological properties of the printing ink

The dynamic viscoelastic properties of the printing pastes with and without pectin were analyzed using a rheometer (MCR301, Anton Paar, Austria) equipped with a serrated parallel plate (gap=1 mm) with a diameter of 25 mm. First, the linear viscoelastic (LVE) region was determined for the sample under oscillation mode. Frequency sweeps were performed over a range of 0.1–10 rad/s within the identified LVE region (strain = 0.1 %). Strain sweeps were also conducted between 0.001 and to 10 % at 1 rad/s and within the LVE. A steady-state flow test was also used for measuring the viscosity when applying a logarithmically increasing shear rate from 0.1 to 500 s^{-1} under rotation mode.

2.5. 3D printing process

A TNO-built extrusion-based 3D printer (Supreme, TNO, The Netherlands) was used for 3D printing. The 30 mL syringe was placed in the syringe holder and connected to the metal nozzle head without applying any heating, and the printing was conducted at 600 mm/min (printer head movement speed in the XY plane) with a nozzle diameter of 1 mm for all the designs. Based on pretrials a specific track width, layer height and extrusion multiplier were chosen for each study, as reported in the following.

2.5.1. Designing and printing model for modifying infill density

To investigate the printability of the fish protein and the effect of pectin an empty cylinder design (diameter=12 mm and height=12 mm) with a track width of 1 mm, layer height of 0.8 mm and extrusion multiplier 1.2 and a flower design with two different extrusion multiplier of 1.2 and 1.5 were printed. To modify infill density, a scaffold model was developed in Rhino CAD software (Rhino 7, Rhinoceros 3D, USA) with fixed dimension of 50 mm in both length and width (see Fig. 1). Then, it was visually programmed in Rhinoceros Grasshopper (Rhino 7, Rhinoceros 3D, USA) to multiply the layers and generate the G-codes. The infill density of the design was modified by changing the number of printing lines in each layer, to achieve infill densities of 25 %, 37 %, 50 %, 75 % and 100 %. The G-codes were saved as VEC files, which were transferred to a TNO developed program called G-Code creator to create the final G-code files including the printing settings. Cubes with different infill density were printed in 4 replicates with a track width of 1.2 mm, layer height of 0.8 mm and extrusion multiplier 1.2. The cylinders, flowers and cubes were immediately subjected to steam cooking (Electric steamer, Philips, The Netherlands) for 5 min, followed by cooling in the fridge (4 °C) for 30 min before conducting the texture analysis.

2.5.2. Designs for development of anisotropic texture

To investigate the possibility of developing anisotropic textures by modifying printing pathways (printing filament direction) in vertical printing layers, the cubes with 100 % infill density were printed once having printing pathways in odd and even layers perpendicular to each other (cross pathway design) or having printing pathways parallel to each other in all layers (parallel pathway design), the latter representing the muscle fibrous structure (Fig. 2). Four replicates from each design were printed with a track width of 1.2 mm, layer height of 0.8 mm and extrusion multiplier 1. The cubes were immediately subjected to steam cooking for 5 min, followed by cooling in the fridge (4 °C) for 30 min before conducting the texture analysis.

2.5.3. Design for texture profiling conceptualization across a single product

A combination of varying infill density and printing pathways were used to engineer a product representing a specific fish like shape in 3D view but having different texture across the internal area of a single printed object (Fig. 3). Printing pathways were chosen and designed in each layer to provide different infill density in the head, neck, belly, caudal, and tail area of the fish to have different texture horizontally across the fish from the head till the tail while still visually representing a fish shape. The design was printed with a track width of 1.7 mm, layer height of 0.6 mm and extrusion multiplier 1.25. The cubes were immediately subjected to steam cooking for 10 min, followed by cooling in the fridge (4 °C) for 30 min before conducting the texture analysis.

2.6. X-ray computed microtomography

The printed cubic samples frozen at −20 °C were analyzed using X-ray computed tomography (CT) to visualize the 3D macro- and microstructure of printed samples. The frozen printed objects were directly placed in a μCT Phoenix VItomeIx M (GE Phoenix v|tome|x m; General Electric, Wunstorf, Germany) having two X-ray sources. The 240 kV micro focus tube with tungsten target was employed. X-rays were produced with a voltage of 110 kV and a current of 110 μA with no filters. The images were recorded by a GE DXR detector array with 2024 × 2024 pixels (pixel size 200 μm). The detector was located 815 mm from the X-ray source and the object was placed 81.6 mm from the X-ray source which resulted in a spatial resolution of 21 μm. A full scan consisted of 1500 projections over 360°. The saved projection was the average of 3 images where every image is obtained over 83 ms exposure time. The 3D images, obtained using the v|tome|x XRT, were analyzed using Avizo imaging software Avizo 3D 2021.2.

2.7. Texture analysis

To evaluate the effect of infill density, each cubic sample was subjected to a uniaxial compression to 40 % of its original height using a cylindrical probe (diameter= 100 mm) moving at the speed of 1 mm/s towards the sample. The sample was placed exactly in the middle of a flat plate attached to the texture analyzer (Universal machines, UK) and the maximum force was recorded and reported as the firmness of the samples. It was presumed that the contact surface area during compression is determined by the dimensions of the probe and the objects which both remained almost constant for all measurements.

To evaluate the effect of printing pathway the cubic samples prinited completely with parallel pathways or with cross pathways in each layer were subjected to a compression to 50 % of their original hieght, using a Warner-Bratzeler flat-end blade. The probe was moving at a speed of 1 mm/s towards the center of the sample. The test was conducted once parallel to the printing paththways, and once perpendicular to the previous direction, and the anisotropy index was caluculated using Eq. (1).

$$\text{Anisotropy index}: \frac{\text{Maximum force in parallel with printing pathway}}{\text{Maximum force perpendicular to printing pathway}} \quad (1)$$

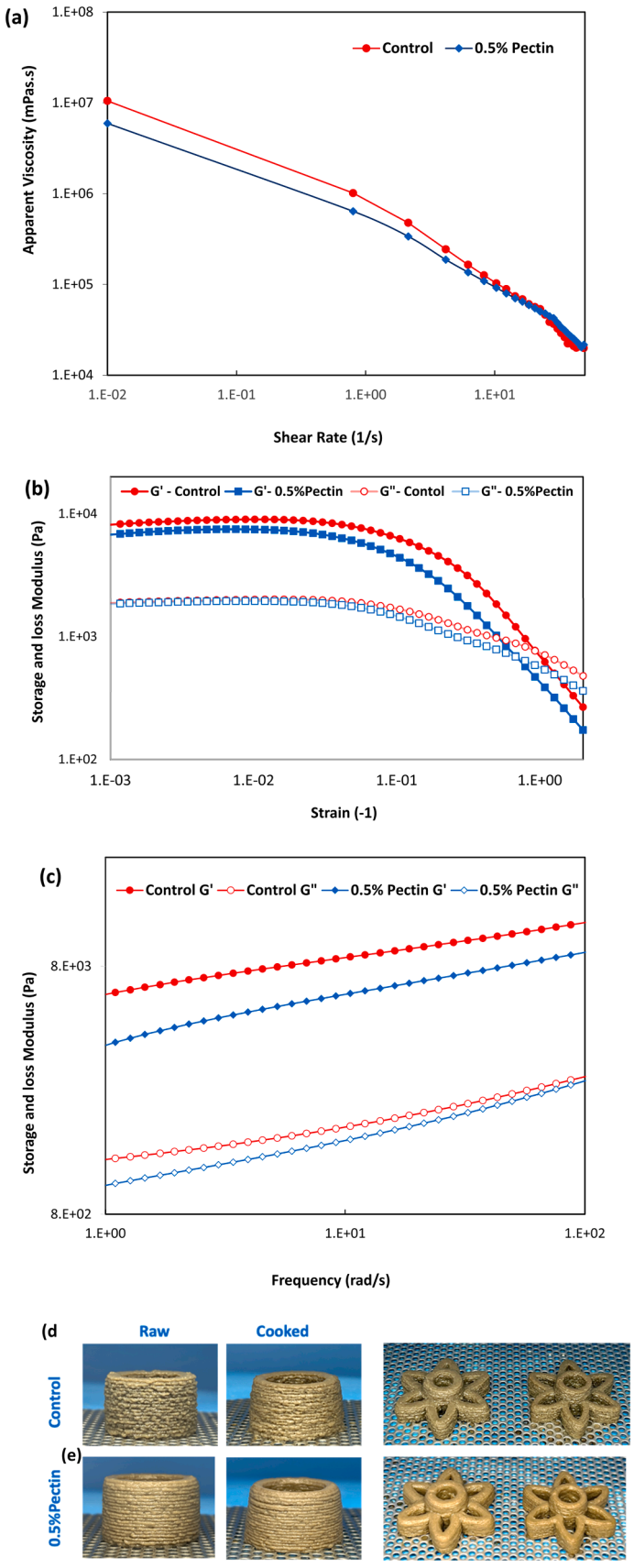

Fig. 4. Flow curve (a), amplitude sweep (b) and frequency sweep (c), 3D printed cylinder and flowers of herring protein isolate (Control) (d) and its combination with 0.5 % pectin (i.e. control + 0.5 % pectin) (e).

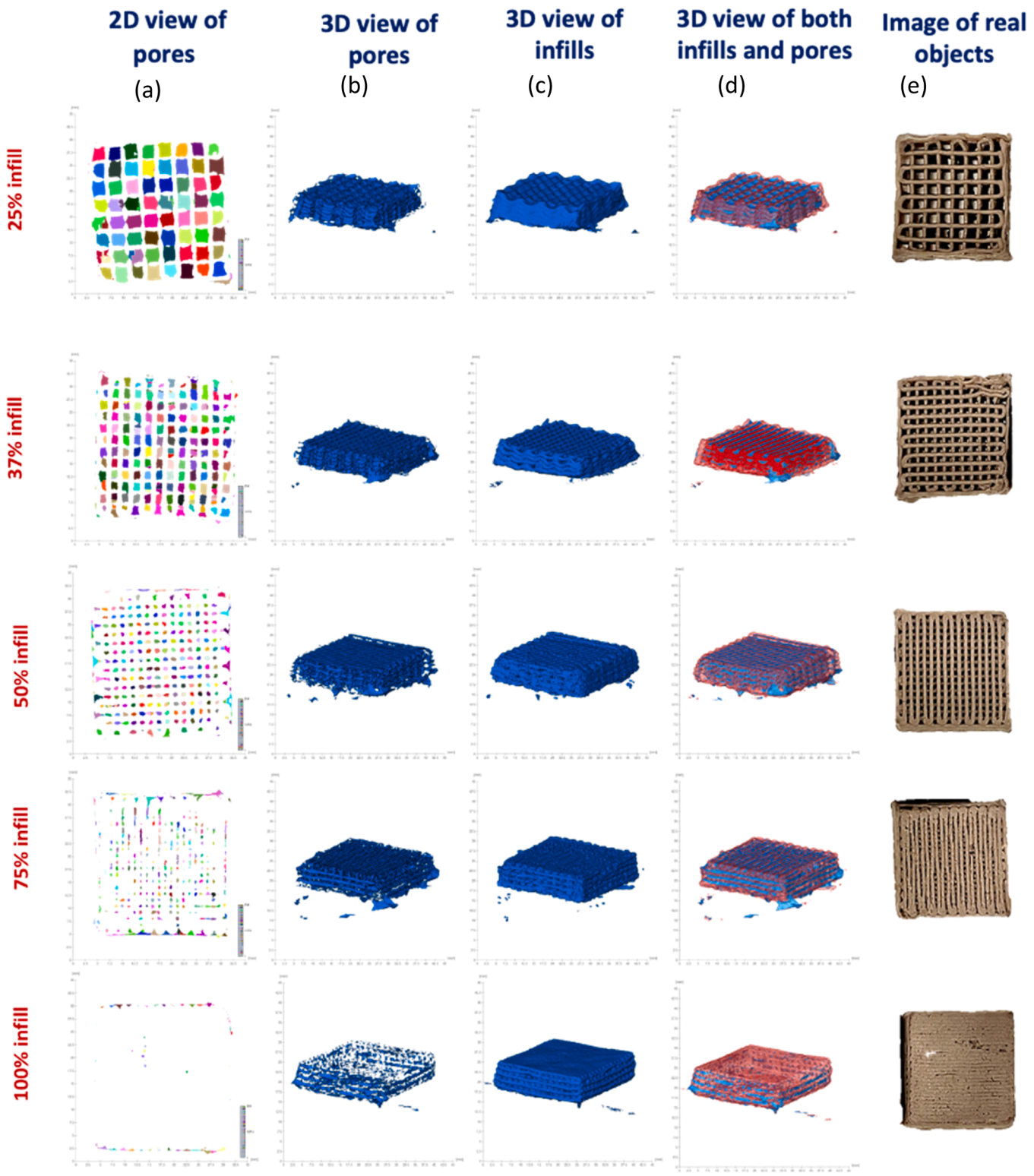

Fig. 5. Micro-CT computed 2D view of pores (a), 3D view of pores (b), 3D view of infills (c), 3D views of both infill zones in red and pores in blue (d) and photographic top view (e) of the printed objects from herring protein isolate (+ 0.5 % pectin) with infill levels of 25 %, 37 %, 50 %, 75 % and 100 %. The void seen in the 100 % infill printed object is partly due to printing imperfections and partly related to image processing.

The texture profile across the printed fish-like object was analyzed at 5 different locations across the sample, representing its head, neck, middle (belly), caudal zone and tail (as shown in Fig. 3) considering the differences in their infill density and printing pathways. Each location was subjected to a uniaxial compression of up to 50 % of the initial height of the location, using a Warner-Bratzeler flat-end blade perpendicular to the length of the fish-like object. The probe was moving at the speed of 1 mm/s towards the center of the sample. The maximum recorded force at each location was considered as the firmness of the area subjected to the cutting.

2.8. Statistical analysis

Statistical analysis was performed using SPSS software (IBM Corp. Released 2021. IBM SPSS Statistics for Macintosh, Version 28.0. Armonk, NY: IBM Corp). The data was evaluated using a one-way analysis of variance (ANOVA) followed by Duncan's multiple range test to determine significant differences between groups. All statistical analyses were performed with a significance level of 0.05, where differences of $p < 0.05$ were considered significant.

3. Results and discussions

3.1. Rheological properties of the protein ink and its formulation

To better understand and optimize the factors affecting the printability of the fish protein isolate, the rheological properties of the protein isolate were measured. The protein isolate was tested in printing of simple objects such as a cylinder and a flower printed with two different extrusion multiplier (Fig. 4d and e). The fish protein isolate formulation showed a relatively high initial viscosity (105×10^2 Pa.s) with a shear thinning behavior. It also had an inherent viscoelastic structure (G'>G") with a yield stress of 1721 Pa. The protein isolate showed a good printability and stand-up (i.e. the ability of a printed object to stand up without collapsing) before cooking, however, some shrinkage after cooking was noticeable. Importantly, the printed objects showed a rough and non- homogenous appearance at their surface before and after cooking which reduced the overall achieved printing accuracy and resolution. To address this issue, 0.5 % of pectin was added to the fish protein isolate which reduced its viscosity to 60×10^2 Pa.s, indicative of a weakening in the primary formed structure in the protein. However, the yield stress remained at 1720 Pa, indicating that still the same minimum stress was required to initiate flow or deformation in the material. These changes in the rheological properties of the protein, provided by the addition of pectin, resulted in a smooth and homogeneous surfaces appearance of the printed objects. Addition of pectin did, however, not manage to mitigate the deformation caused by steam cooking. Although hydrocolloids are widely used and studied as assistant agents to improve the printability of different types of food and food ingredient such as proteins (Chen et al., 2022; Fan et al., 2022), still very little is known about the effect of pectin. Depending on the pectin type, its concentration, medium pH, temperature, ionic strength etc., the type of interactions between pectin and proteins will be different (Buda et al., 2021; Gonza, 2002; Mishra et al., 2001) which will in turn define the rheological properties of a protein paste. It seemed that when 0.5 % of pectin was added to the herring protein paste, which already had a relatively good protein network, it just interfered with the protein network structure in the paste. This interference disrupted and weakened the protein-protein interactions, causing the observed series of changes in the viscoelastic properties of the fish protein paste or acted a lubricating agent. Hereby, it facilitated the flowability and deformability of the paste, during and after extrusion through the nozzle, and adaptation to the printing pathways. Reduction of viscosity without reducing yield stress turned out to be a desired outcome for improving the overall accuracy and resolution of the printed protein filaments during 3D printing, without jeopardizing the stand-up and structural integrity of the printed object.

3.2. Tuning texture via modifying infill density

As can be seen in Fig. 5e, with almost all infill desnities, the samples managed to keep their cubic shape and layers could stand on top of each other, resulting in a shape that closely resembles the overall 3D design. After cooking, all the samples had an elastic texture and could be manually handled without collapsing. However, with decreasing infill density, the number of mismatches between the location of printed fibers (filaments) and the original design path increased, especially in objects with a 37 % and 25 % infill density. The reasons for this are: (1) at lower infill densities (≤37 %) a weak mechanical structure was formed, which could not fully support the load of the upper layers, especially on the edges and (2), the low amount of material resulted in a low surface area between the layers for adhesion, which is important for achieving a good accuracy and resolution. This is in line with results previously reported (Liu et al., 2018) when printing mashed potato objects with low infill densities. The micro-CT imaging (Fig. 5a–d) also confirmed that the porosity level in the printed objects was different, depending on the used infill density, and showed that it was preserved after cooking. This means that the structures did not collapse during or after printing, including during the cooking process.

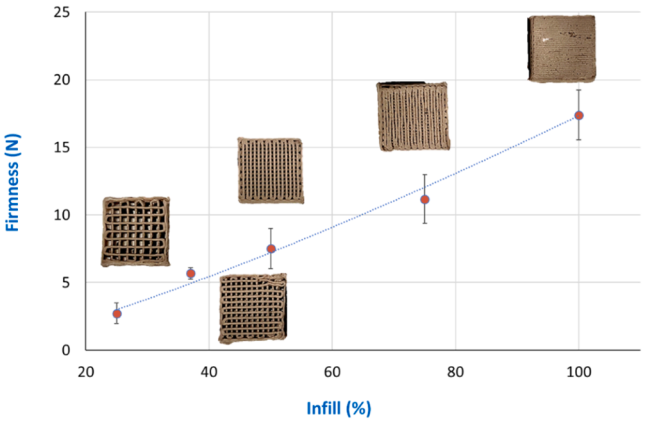

Fig. 6. Effect of infill density on uniaxial firmness of printed cubes from herring protein isolates (+0.5 % pectin) and the representative picture of the printed cubes from herring protein isolates with infill densities ranging from 25 to 100 %.

As can be seen in Fig. 6, changing the infill density has a significant effect on the textural properties of the printed objects. Decreasing the infill density resulted in a decrease in the firmness of the samples in an almost linear manner (R^2=0.986). Decreasing the infill density from 100 % to 75 % and 50 % reduced the firmness of the printed objects from 17 N to 11 and 7 N, respectively. Further reduction of the infill density to 37 % and 25 % reduced the firmness of the samples to 5.2 and 2.5 N, respectively. Since the infill design and the wall thickness of the internal pores were constant in the printed object, the changes in the infill density showed a clear correlation with their textural properties. This was mostly because the infill density defines the amount of material (the protein gel) in the object which should handle the uniaxial stress applied during the compression test. This can open up new opportunities for tailoring and customizing the textural properties of gel-based products using 3D printing by simply changing the infill density. The findings are in line with previous observations for 3D printed hard food products such as cookies (Piovesan et al., 2020) and gums (Adedeji et al., 2022) cereal snacks (Derossi et al., 2020), as well as for 3D printed soft food products such as mashed potato shapes (Liu et al., 2018; Liu and Zhang, 2021), where an inverse correlation between the hardness/firmness of the printed products and their infill density was observed. In a most relevant example, changing infill density scaffolds printed from an abalone protein paste from 20 to 80 % filled with gelatin was found very effective in producing foods with different hardness for elderly people (Yun et al., 2023).

3.3. Anisotropic texture development via printing pathway

The effect of printing pathway in parallel and cross-mode in different printing layers in Z axis on the visual appearance of printed cubes and their tomography-derived microstructure can be seen in Fig. 7a. The overall cube shape of the design was recreated using both printing modes, regardless of the used printing path. However, the external

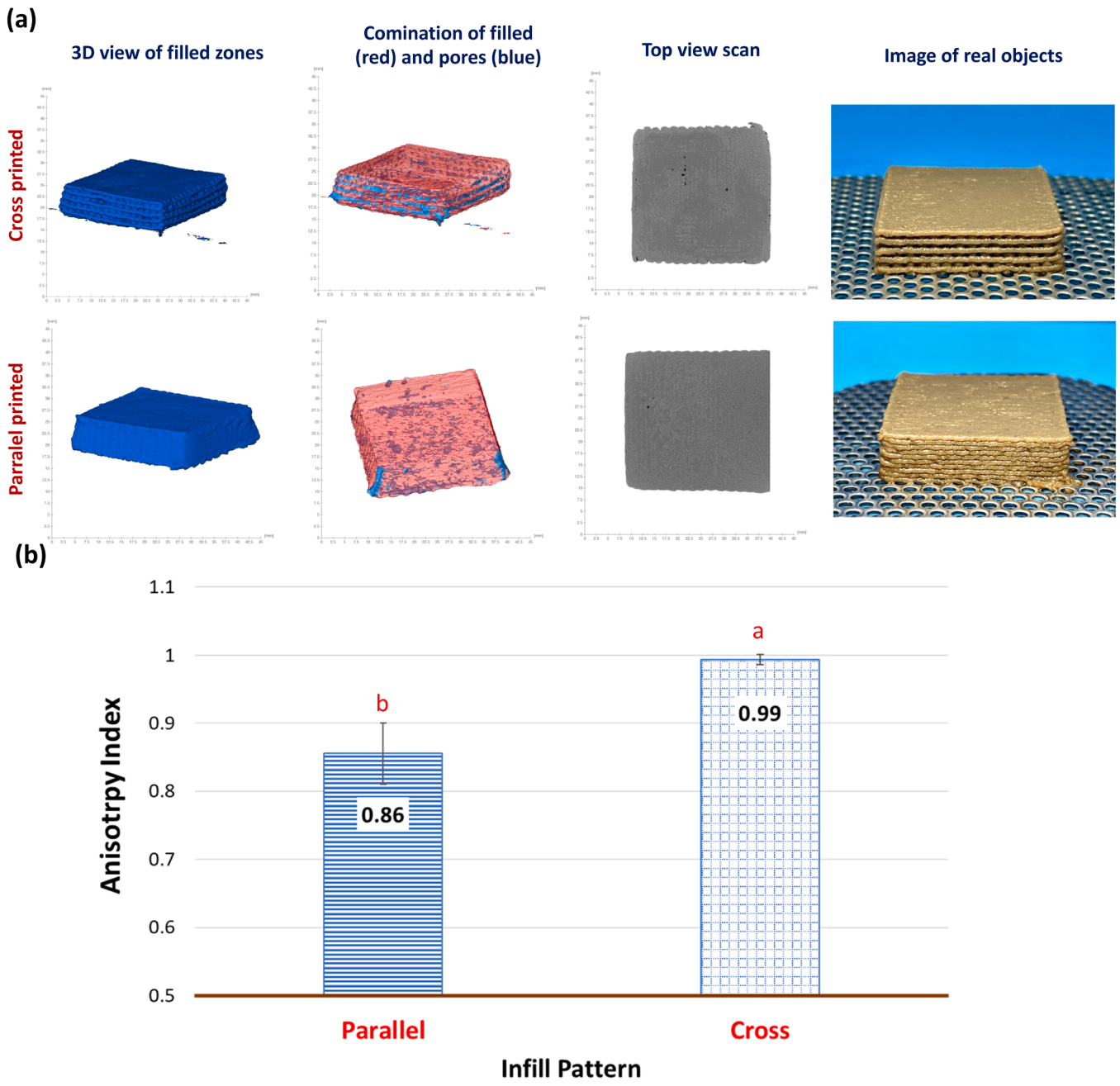

Fig. 7. Representative (a) 3D micro-CT computed view of filled parts (column 1), combination of filled and pores (column 2), top view scan of the objects (column 3) and photographic side view (column 4) and (b) anisotropy index of the cubes printed from herring protein isolate (+0.5 % pectin) with parallel and cross pathways across the Z-axis.

appearance of the sample from the side views (Fig. 7a column 4) was slightly affected by the two printing pathways. This is mostly due to the difference in the amount of material deposited at the end of each printing line and how they differ with the line from the previous layer. The micro-CT imaging (Fig. 7a columns 1–3) did not show any difference in the internal structure of the samples in terms of infill density and their overall geometry.

The results for the anisotropy index (AI), calculated based on applying uniaxial cutting in two different perpendicular directions relative to the printed strand, are shown in Fig. 7b. The difference between the two cutting forces was represented as the anisotropy index. In this case, a value of 1 indicates uniform texture or isotropic texture, while values above or below 1 show anisotropy in the texture. The larger the difference between the two cutting forces, the more anisotropic the texture is, which may indicate the presence of a fibrous texture and muscle-like textural properties (Osen et al., 2014). As can be seen, the sample printed using the cross pathways between the layers showed an AI of 0.99, meaning a homogenous or isotropic texture. The samples printed using the parallel path in all layers, however, showed an AI of 0.86 which was significantly ($p < 0.5$) lower, indicating anisotropy and texturization in the samples. This is mostly related to the lower amount of cutting force needed when applying the cutting in parallel with the printing path compared with the cutting force needed when applying the uniaxial force perpendicular to the printing path in the Z axis. The effect of the printing path on the anisotropy of gel-based or protein-based products has not been reported before. However, it has been previously shown that parallel printed products made of alginate-containing pea proteins or single cell proteins (Calton et al., 2023) and surimi and

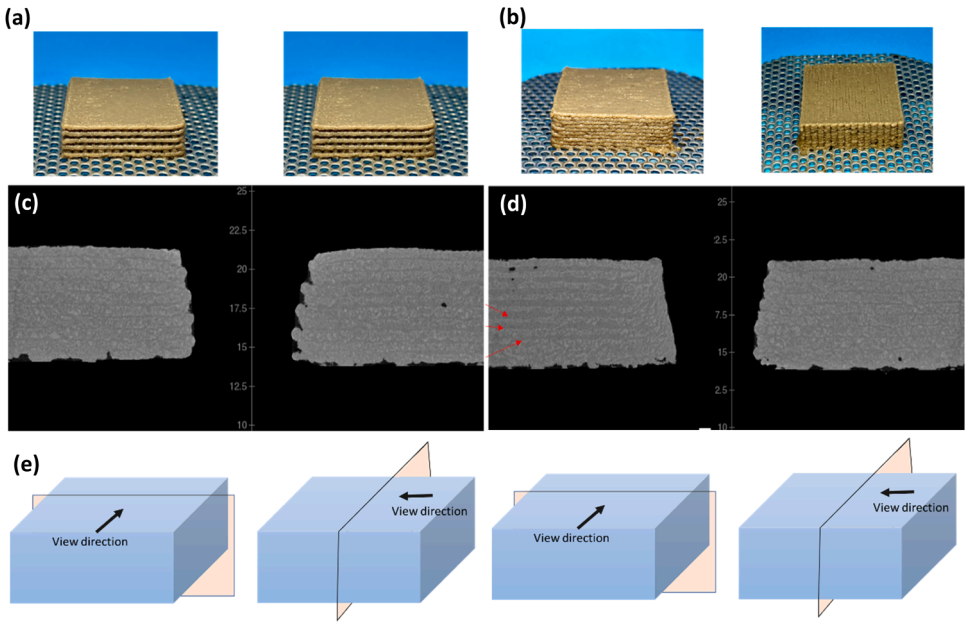

Fig. 8. Representative photographic side view of the cubes printed with cross (a) and parallel (b) pathways across their z-axis and, micro-CT images of the x-axis and y-axis slices of the samples printed with cross (c) and parallel (d) pathways from herring protein (+ 0.5 % pectin) and the direction views (e). The red arrows show the difference in the material disposition amount at the interface of the printing layers.

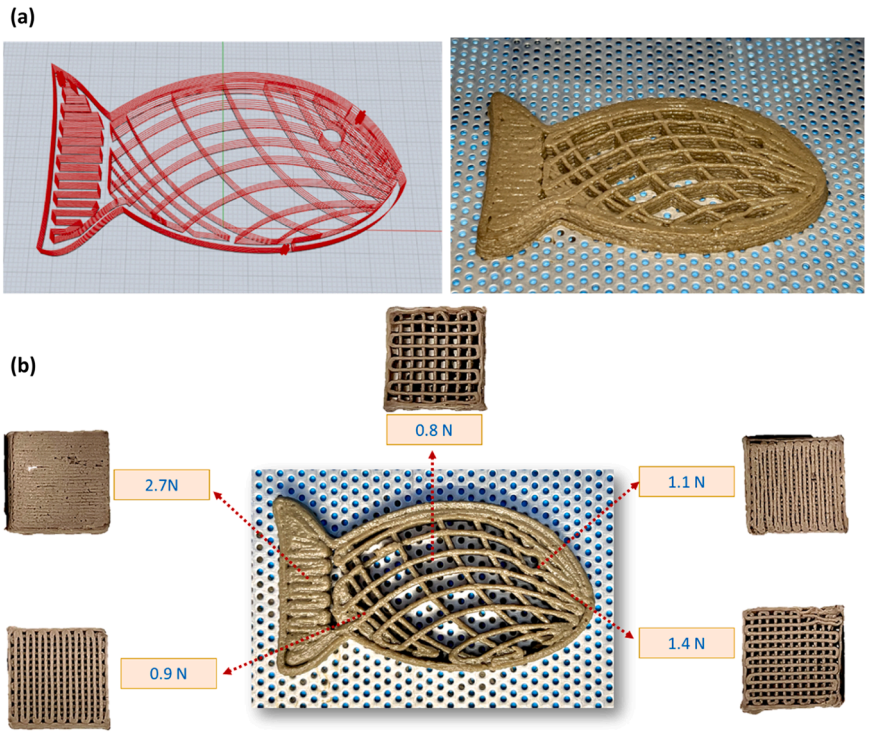

Fig. 9. Representative (a) side view of the 3D model of the designed fish and its final printed form from herring protein isolate (+0.5 % pectin) (b) average uniaxial firmness (cutting force) measured in different parts of the fish, and the type of texture that they represent.

plant-protein based products printed using different deposition patterns in each layer (Lee et al., 2023) showed higher anisotropy compared with molded products with the same composition when assessed with bi-directional cutting.

X-ray microtomography images of x-axis and y-axis slices of the samples (Fig. 8) printed using cross pathway did not show any vertical difference in terms of distribution and deposition of the materials at the interface of the printing layers (see Fig. 8c). However, when looking at the samples printed using parallel printing pathways, all the layers showed lower amounts of protein material at the interface of the printing filaments in the sequential layers (lower protein density) in the X-ray microtomography image taken parallel to the printing path compared with the X-ray microtomography image taken perpendicular to the printing pathways (see red arrows on Fig. 8d). This could explain the anisotropic behavior found in the samples with parallel printing pathway, which is related to differences in the amount of protein

deposited in different sections of the samples while a homogenous load of material was created using the cross-printing pathway between the layers. This is in line with the inherent anisotropic nature of almost all 3D printed objects when studied in parallel with the printing platform or in-plane direction and compared with the build direction due to their layer by layer structure (Piovesan et al., 2020). It seems that a layer by layer structure was created when all the printing paths were aligned vertically. Jonkers et al. (2022) showed that there is a direct relationship between the mechanical properties of the objects printed by using the selective laser sintering process and their energy density, which is defined by their material density when subjected to uniaxial stresses in the build direction and the principal in-plane direction.

3.4. Texture profiling conceptualization

As can be seen from the overall appearance of the printed object shown in Fig. 9, it was possible to print a product with different infill densities and printing pathways across the length of the product but keep its overall shape like a fish even after cooking. The printed object had a very good agreement to the designed digital model too. The texture analysis results showed different firmness at different parts of the fish, depending on the infill density in each part. The tail, having the highest infill density and parallel printing and created using a parallel printing pathway, showed the highest firmness (2.27 N), which was followed by the head (1.4 N), neck (1.1 N), caudal zone (0.9 N), and belly (0.8 N) of the fish, correlating with the infill density in each zone. These results prove that it is possible to engineer the texture profile across a protein-based product by changing infill density and printing pathways to produce printed foods closer to real food products, which are normally very heterogenous in their texture in different parts, such as a fish fillet. This can also introduce new opportunities for customization and personalization of food products in terms of texture via 3D printing. Derossi et al. (2022) showed the possibility of using 3D printing to mimic apple texture, as an example of plant tissue, across the X and Y axis in a cereal based snack using the morphological information of apple tissue obtained from microtomographic images. They managed to achieve different textures in different parts of the snack architecture by changing porosity level in a heterogeneous or unparalleled form in X and Y axis directions (unlike the cubes) as achieved in our study.

4. Conclusions

The feasibility of using 3D printing for structure design to engineer the texture of gel-based seafood products was explored. Adjusting infill density was a very effective approach to adjust and customize the textural properties of 3D printed products made from this type of proteins. A direct correlation between the infill density and uniaxial firmness of the printed objects was found. However, objects with an infill density lower than 35–37 % showed lower agreement with the 3D design after cooking due to low material deposited in each layer. Using parallel printing pathways vs cross printing between the layers was also found as a novel approach for modifying the texture of the protein-based printed products. Parallel printing pattern resulted in anisotropic textures which was explained by the nonhomogeneous load of materials in parallel with the printing pathways compared with its perpendicular direction as revealed by microtomography imaging. Cross printing pathway design resulted in isotropic textures. Finally, it was demonstrated that a combination of filling density and printing pathways can be used across the X and Y-axis of a single product in a unparallel manner to achieve different structures and architectures in different parts of a single product. This allows for texture profiles in 3D printed products which have the heterogeneous nature of actual foods, but also provide new opportunities for development of protein-based products with customized and personalized textures using the 3D printing technology.

Statement of human and animal rights

There has not been any studies conducted on human or live animal in the submitted work.

CRediT authorship contribution statement

Mehdi Abdollahi: Writing – review & editing, Writing – original draft, Visualization, Validation, Software, Methodology, Investigation, Funding acquisition, Formal analysis, Data curation, Conceptualization. **Maaike Nieuwland:** Writing – review & editing, Methodology, Formal analysis, Data curation. **Kjeld van Bommel:** Writing – review & editing, Supervision, Resources. **Laurice Pouvreau:** Writing – review & editing, Supervision, Resources. **Anna Ström:** Writing – review & editing, Funding acquisition. **Ingrid Undeland:** Writing – review & editing, Resources, Project administration, Funding acquisition, Conceptualization.

Declaration of competing interest

The authors declare the following financial interests/personal relationships which may be considered as potential competing interests:

Mehdi Abdollahi reports financial support was provided by Sweden's Innovation Agency. Ingrid Undeland reports financial support was provided by Horizon Europe.

Acknowledgment

We are thankful to FORMAS, the Swedish Research Council, for the financial support of the research (CROSS project# 2016-00246 and 3DMix project# 2021-02349). Thanks to Sweden Pelagic AB for providing herring by-products. Part of the presented results are obtained using X-ray tomography equipment which is owned by Shared Research Facilities and subsidized by Ministry of Economic Affairs and the province of Gelderland, The Netherlands.

Data availability

Data will be made available on request.

References

Abdollahi, M., Wu, H., Undeland, I., 2021. Impact of processing technology on macro- and micronutrient profile of protein-enriched products from fish backbones. Foods 10 (5), 950. **2021**.

Adedeji, O.E., Choi, J.Y., Park, G.E., Kang, H.J., Aminu, M.O., Min, J.H., Chinma, C.E., Moon, K.D., Jung, Y.H., 2022. Formulation and characterization of an interpenetrating network hydrogel of locust bean gum and cellulose microfibrils for 3D printing. Innov. Food Sci. Emerg. Technolog. 80, 103086. https://doi.org/10.1016/J.IFSET.2022.103086.

Buda, U., Priyadarshini, M.B., Majumdar, R.K., Mahanand, S.S., Patel, A.B., Mehta, N.K., 2021. Quality characteristics of fortified silver carp surimi with soluble dietary fiber: effect of apple pectin and konjac glucomannan. Int. J. Biol. Macromol. 175, 123–130. https://doi.org/10.1016/j.ijbiomac.2021.01.191.

Calton, A., Lille, M., Sozer, N., 2023. 3-D printed meat alternatives based on pea and single cell proteins and hydrocolloids: effect of paste formulation on process-induced fibre alignment and structural and textural properties. Food Res. Int. 174 (P2), 113633. https://doi.org/10.1016/j.foodres.2023.113633.

Chen, Y., Zhang, M., Sun, Y., Phuhongsung, P., 2022. Improving 3D/4D printing characteristics of natural food gels by novel additives: a review. Food Hydrocoll. 123 (July 2021), 107160. https://doi.org/10.1016/j.foodhyd.2021.107160.

Dadbakhsh, S., Vrancken, B., Kruth, J.-P., Luyten, J., Van Humbeeck, J., 2016. Texture and anisotropy in selective laser melting of NiTi alloy. Mater. Sci. Eng.: A 650, 225–232.

Derossi, A., Caporizzi, R., Paolillo, M., Severini, C., 2020. Programmable texture properties of cereal-based snack mediated by 3D printing technology. J. Food Eng. 289 (December 2019), 110160. https://doi.org/10.1016/j.jfoodeng.2020.110160.

Derossi, A., Paolillo, M., Verboven, P., Nicolai, B., Severini, C., 2022. Extending 3D food printing application: apple tissue microstructure as a digital model to create innovative cereal-based snacks. J. Food Eng. 316 (October 2021), 110845. https://doi.org/10.1016/j.jfoodeng.2021.110845.

Fan, Z., Cheng, P., Zhang, P., Zhang, G., Han, J., 2022. Rheological insight of polysaccharide/protein based hydrogels in recent food and biomedical fields: a

review. Int. J. Biol. Macromol. 222 (PB), 1642–1664. https://doi.org/10.1016/j.ijbiomac.2022.10.082.
Gonza, J.J., 2002. Effect of Pectins on the Gelling Properties of Surimi from Silver Carp, 16.
Jonkers, N., van Dijk, W.J., Vonk, N.H., van Dommelen, J.A.W., Geers, M.G.D., 2022. Anisotropic mechanical properties of Selective Laser sintered starch-based food. J. Food Eng. 318 (October 2021), 110890. https://doi.org/10.1016/j.jfoodeng.2021.110890.
Lee, S.H., Kim, H.W., Park, H.J., 2023. Integrated design of micro-fibrous food with multi-materials fabricated by uniaxial 3D printing. Food Res. Int. 165 (August 2022), 112529. https://doi.org/10.1016/j.foodres.2023.112529.
Lipton, J.I., 2017. Printable food: the technology and its application in human health. Curr. Opin. Biotechnol. 44, 198–201. https://doi.org/10.1016/j.copbio.2016.11.015.
Liu, Z., Bhandari, B., Prakash, S., Zhang, M., 2018. Creation of internal structure of mashed potato construct by 3D printing and its textural properties. Food Res. Int. 111 (March), 534–543. https://doi.org/10.1016/j.foodres.2018.05.075.
Liu, Z., Dick, A., Prakash, S., Bhandari, B., Zhang, M., 2020. Texture modification of 3D printed air-fried potato snack by varying its internal structure with the potential to reduce oil content. Food Bioproc. Tech. 13 (3), 564–576. https://doi.org/10.1007/s11947-020-02408-x.
Liu, Z., Zhang, M., 2021. Texture properties of microwave post-processed 3D printed potato snack with different ingredients and infill structure. Future Food. 3, 100017. https://doi.org/10.1016/J.FUFO.2021.100017.
Mantihal, S., Prakash, S., Bhandari, B., 2019. Texture-modified 3D printed dark chocolate: sensory evaluation and consumer perception study. J. Text. Stud. 50 (5), 386–399. https://doi.org/10.1111/jtxs.12472. Issue.
Mishra, S., Mann, B., Joshi, V.K., 2001. Functional improvement of whey protein concentrate on interaction with pectin. Food Hydrocoll. 15 (1), 9–15. https://doi.org/10.1016/S0268-005X(00)00043-6.
Oppen, D., Grossmann, L., Weiss, J., 2022. Insights into characterizing and producing anisotropic food structures. Crit. Rev. Food Sci. Nutr. 0 (0), 1–19. https://doi.org/10.1080/10408398.2022.2113365.
Osen, R., Toelstede, S., Wild, F., Eisner, P., Schweiggert-Weisz, U., 2014. High moisture extrusion cooking of pea protein isolates: raw material characteristics, extruder responses, and texture properties. J. Food Eng. 127, 67–74. https://doi.org/10.1016/j.jfoodeng.2013.11.023.
Piovesan, A., Vancauwenberghe, V., Aregawi, W., Delele, M.A., Bongaers, E., de Schipper, M., van Bommel, K., Noort, M., Verboven, P., Nicolai, B., 2020. Designing mechanical properties of 3d printed cookies through computer aided engineering. Foods 9 (12). https://doi.org/10.3390/foods9121804.
Yun, H.J., Jung, W.K., Kim, H.W., Lee, S., 2023. Embedded 3D printing of abalone protein scaffolds as texture-designed food production for the elderly. J. Food Eng. 342, 111361. https://doi.org/10.1016/J.JFOODENG.2022.111361.
Zhu, S., Ruiz de Azua, I.V., Feijen, S., van der Goot, A.J., Schutyser, M., Stieger, M., 2021. How macroscopic structure of 3D printed protein bars filled with chocolate influences instrumental and sensory texture. Lwt 151 (May), 112155. https://doi.org/10.1016/j.lwt.2021.112155.